JOURNAL OF OPTOELECTRONICS AND ADVANCED MATERIALS Vol. 9, No. 7, July 2007, p. 2156 - 2161

All-optical poling in a new cross-linkable polymer system based on melamine

B. GUO[a,b*], F. S. LIU[b], Y. CHEN[b], Z. Y. LUO[b], L. J. ZHU[b], Y. J. JIA[c], G. M. WANG[c]
[a]*Laboratory of Solid State Microstructures, Nanjing University, Nanjing 210093, China.*
[b]*College of Information Science and Technology, Nanjing Forestry University, Nanjing 210037, China*
[c]*Department of Optical Science and Engineering, Fudan University, Shanghai 200433,China*

All-optical poling of crosslinkable polymer systems based on hexamethoxymethyl melamine (HMMM) and Disperse red 1 and 19 were experimentally investigated. Optimum poling condition of the two seeding beam intensity ratio, the temperature dependence, and the temporal stability of them were studied in details. It was found that the saturation SHG intensity decreased significantly with the increase of the sample temperature from 33 ^{o}C to 63 ^{o}C. From the respect of energy balance, the main factors of all-optical poling were analyzed, and a simple equation was first deduced to describe the requirement of realizing all optical poling.

(Received December 11, 2006; accepted June 27, 2007)

Keywords: All-optical poling, Azobenzene, Melamine

1. Introduction

Macroscopic non-centrosymmetric structure is the requirement to achieve second-order nonlinear optical (NLO) effect, which has been extensively studied for the applications in electro-optical (EO) modulation and frequency-conversion device. At present, several chromophore orientation techniques have been developed to realize this noncentrosymmetric structure. They are: electric field poling; photoassisted poling; and all optical poling. Among them, all optical poling has many desirable features over the others, such as, phase matching for SHG can automatically be achieved, no electrodes are required, and micropattering of the second order susceptibility can be simply achieved by scanning the focal area over the sample surface [1].

Considering actual device applications, NLO polymeric materials should possess long-term stability, high physical and mechanical stability, and low optical propagation loss. In the case of temporal stability, introducing a thermosetting polymer system was manifested to be efficient to stabilize the oriented chromophores. Xu et al. first introduced the concept of thermal crosslinking into optical poling in polyurethane systems [2,3]. Besides this, Si et al. reported another thermosetting polymer of thermal-imidization polyimide with disperse red 19 pendant groups [4]. In all of them, NLO chromophore was effectively restricted in matrix; hence, the stability properties of optically induced polar orientation were greatly improved.

Melamine-based materials have been widely used in the lighting, coating, and decorating industries because of their good transparency. Jeng et al. reported the first complete study on melamine-based polymers by sol-gel process [5], their results showed that these materials with low optical loss, high Tg, and cross-linked features are good candidates for the second-order NLO system. Much work has been done in this area [6-8], however, to the best of our knowledge, their poling orientation are all realized under electric field. In this work, we first introduced optical poling into this material and had a preliminary study concerned with its all-optical poling behavior. Combined the characteristic that can be automatically achieved phase matching for SHG from all optical poling, with the low optical loss and cross-linked features from this materials, we expect this system will be promising in frequency doubling waveguide devices.

Resimene747 resins being primarily HMMM from Solutia are amino crosslinkers designed for thermosetting surface coatings. Their principal function is to crosslink the molecules in a coating to form a three-dimensional thermoset polymer network. Here, azobenzene chromophores DR-1 and DR-19 with reactive group of hydroxyl were incorporated into the matrix based on prepolymer of HMMM by sol-gel process. Optimum poling condition of the two seeding beam intensity ratio, the temperature dependence of all-optical poling process were studied in details, furthermore, the requirement of realizing all optical poling was first deduced according to the energy balance. Finally, the temporal stability, i.e., the SHG relaxation behaviors of these melamine-based NLO materials also have been studied by the mono-exponential function, compared with typical guest-host system of PMMA/DR-1.

2. Experimental

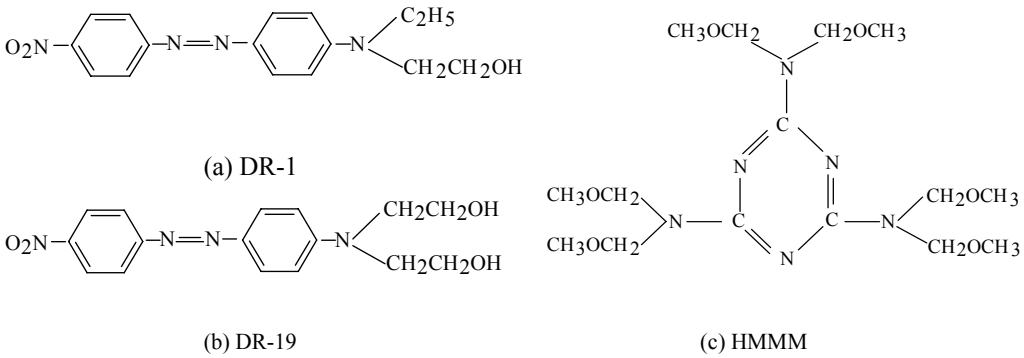

Fig. 1.Chemical structures of: (a) DR-1; (b) DR-19; and (c) HMMM.

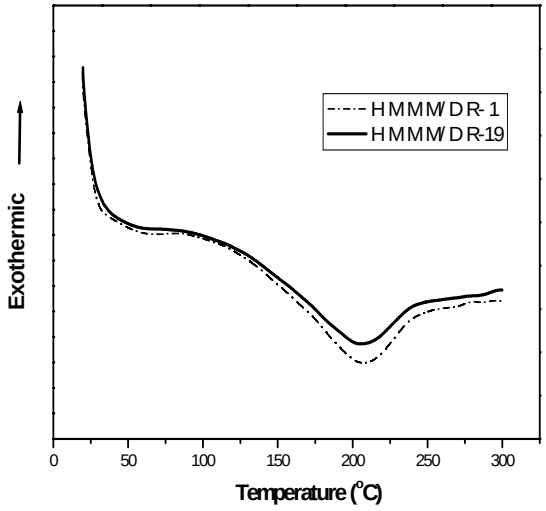

Fig. 2. DSC of cured HMMM/DR-1 and DR-19 at 120℃ for 1 h.

Disperse red 1 and 19 (ACROS ORGANICS) were recrystallized from ethanol. HMMM (Resimene747) was from Solutia and was used as received. Fig. 1 shows their chemical structure. The prepolymer of HMMM was prepared by heating the monomer at 60℃ for 12 h, then 80℃ for 12 h in the presence of an acid catalyst. The prepolymer of HMMM (0.9 g) and Disperse red dye (0.1g) was dissolved in cyclopentanone with water (0.1g) and acetic acid (0.1 g) to aid the hydrolysis of the prepolymer. This solution was stirred for 1 h at room temperature, and then was filtered through a 0.2 μm Teflon membrane. Finally, thin film was made by spin coating on glass substrates. By adjusting the revolutions per minute of the spin coater, the sample thickness was controlled at about 1μm. The DR1-doped pure PMMA (1% mass ratio) film was also fabricated by spin coating.

The curing condition was chosen to be 120℃ for 1 h , the major cross-linking reaction was shown in equation (1), which results in the loss of –OH and $–OCH_3$ groups to form an ether cross-link and liberate methanol [9].

$$-NCH_2OCH_3 + ROH \overset{H^+}{\rightleftharpoons} -NCH_2OR + CH_3OH$$

The T_g was determined by Differential scanning Calorimetry (DSC), which was performed on a Shimadzu DT-50 thermal analyzer under nitrogen flow in a range from room temperature to 300 °C, and the heating rate was 10°C · min-1. Film thickness was measured with an Alpha-Step 500 Surface Profiler.

The experimental setup of all-optical poling is reported in literature in details [2]. An oven was added to control the sample temperature in the process of poling. During the whole all-optical poling processes, no obvious photodestruction occur in the films. The Second-order NLO coefficient d_{33}, was evaluated by use of a Y-cut quartz crystal as the reference material, for which a value of d_{11} = 0.5 pm/V was assumed.

A mode-locked Nd:YAG laser beam was used operating at 1064 nm with a pulse width of 36 ps ,pulse energy 1mJ,and 10 Hz repetition rate. The beam waist diameter at the sample location was 2 mm. A KTP (KTiOPO4) crystal was used as the frequency doublers.

3. Results and discussion

3.1 Optimum poling condition of the two seeding beam intensity ratio

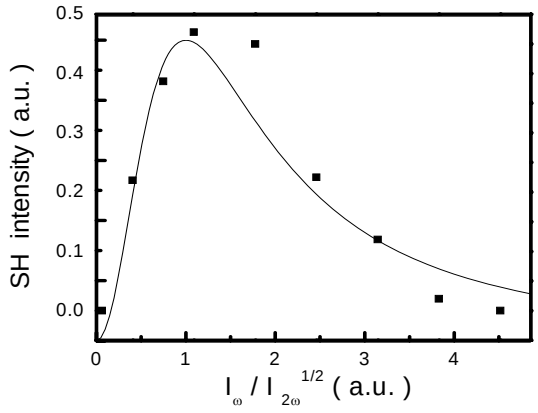

Fig. 3. SH intensity against the different intensity ratio.

Many factors were often considered in all optical poling process, such as, time of seeding, the phase difference and the intensity ratio between $\omega$and 2ω seed beams[10]. In this study, the sample HMMM/DR-1 of 1μm was used, the poling time was for 1 hour, we studied the optimum poling condition for the intensity ratio of the two seeding beam under room temperature. The relation between the generated SH intensity and the relative intensity can be expressed as a parameter, $R = I_\omega \Big/ I_{2\omega}^{1/2}$. As is shown in Fig. 3, the strong dependence of the generated SH intensity on the intensity ratio between ω and 2ω was observed. The maximum SH intensity was obtained at R=1, and the d_{33} was estimated to be 2.5 pm/V.

According to the literature [10,11], at a given phase difference, the photo-induced SH intensity can be determined by the following three terms: the one-photon absorption at 2ω, the two photon absorption at ω, and the interference between$\omega$and 2ω, which is proportional to $I_{2\omega}$, I_ω^2,and $I_\omega I_{2\omega}^{1/2}$, respectively. The relationship of them is given by the following equation [11]:

$$I_{2\omega} \propto \left(\left| I_\omega I_{2\omega}^{1/2} \right| / \left| I_\omega^2 + \gamma I_{2\omega} \right| \right)^2 = \left[R / \left(R^2 + \gamma \right) \right]^2 \quad (2)$$

where $R = I_\omega \Big/ I_{2\omega}^{1/2}$ and γ is a proportionality factor depending only on the dipole moment difference between the ground states and excited states of the nonlinear molecules in the case of two-level model.

The solid curve in Fig. 3 is the fitting result given by equation (2). The agreement between the theoretical fit and experimental data is fairly good.

3.2 The temperature dependence of DR1–HMMM film in all-optical poling

Four different temperatures of 33~63℃ were carried out in the optical poling for HMMM/DR-1 film. The poling processes are shown in Fig. 4. It can be found that the induced saturation SHG intensity decreased significantly with the increase of the sample temperature from 33℃ to 63℃, the maximum saturation SHG intensity at 33℃ is about 5 times larger than at 53℃. Moreover, when the poling temperature attained to 63℃, no SHG signal was observed.

Recently, Fiorini etc. have established a theory [12], whose important result is that the optimization of all-optical poling relies not only on the optical seeding conditions but also on the chemical physics process of the polymer matrix. They introduced a parameter $\overline{D} = D/(\xi B)$ to describe the influence of the ratio between spontaneous and photoinduced reorientation diffusion rates [12]. ξ is the quantum efficiency for molecular reorientation, B is the excitation rate due to the two-photon absorption at frequency ω, they also presented the equation as follows:

$$\chi^{(2).sat} \propto \frac{1}{36 + 70\,\overline{D}} \quad (3)$$

Here, the significant change can be related to the orientation diffusion constant D caused by temperature. According to the equation above, we can explain the experimental results qualitatively: as the temperature was varied from 33℃ to 63℃ in all-optical poling, the orientation diffusion constant D increased rapidly. Assume that ξ and B is almost constant in this temperature range, then $\overline{D}$ also increased. Finally, the saturation $\chi^{(2).sat}$, i.e. the saturation photoinduced SHG decreased significantly.

In general, the saturation SHG is sensitive to the range of temperature mentioned above, though which is much lower than the glass transition temperature about 155℃ (Fig. 2.). This result is different from the thermal-assisted optical poling of disperse red 19 functionalized polyimide side-chain polymer (Tg ≈190 °C)[13], whose saturation SHG increase with the increase of poling temperature, and the diffusion constant D was believed to be constant at a temperature range much lower than the Tg [14]. This drastic difference maybe ascribed to the micro porous

structure in the cross-linked HMMM/DR-1 films resulted from liberating small molecules in cure reactions, which in turn resulted in significant increase of the orientation diffusion constant D, even though from 33℃ to 63℃. Further verification and study is now in progress. Similar results were also observed in HMMM/DR-19 films.

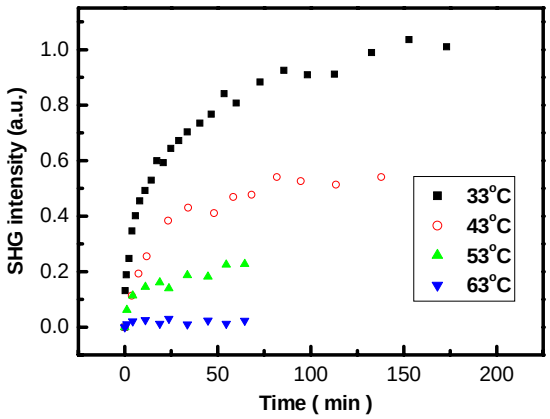

Fig. 4. SHG intensity at the different poling temperature in HMMM/DR-1.

3.3 The requirement to realize all optical poling

For the potential applications of all-optical poling, understanding the all-optical poling process is necessary. According to the analysis above, two competing parameters of spontaneous orientation and photoinduced orientation diffusion rates were proposed and verified to govern the microscopic all-optical orientation process. However, what we interested is to answer what condition is required to realize the all-optical poling for a specific matrix, based on the above two competing factors. Otherwise to previous reports [10,12], the opinion of energy equilibrium will be applied to analyze the main factors of all-optical poling.

From Fig. 4, on the one hand, the temperature dependence shows obviously the differences of poling process under different temperatures in this cross-linked system; on the other hand, it also revealed that 63℃ is the critical point where the energy equilibrium occurs between the energy of making NLO molecules orientation from optical field *E* and the random thermal motion energy of DR-1 under this specific temperature.

For a NLO molecule, when it was oriented by polar optical field *E*, the corresponding energy can be expressed as μE (μ is dipole moment), in which the unit is joule. In the same time, the orientation diffusion process is mainly related to thermal randomization energy, by introducing the classical ideal gas model, thermodynamic function *U* of internal energy can be obtained by partition function. Thus, if □E ≥ U, then, the all optical poling can be realized.

The light intensity I at the sample location can be calculated to be 8.85×1012 J·m-2·s^{-1} .

Also, the relation of Light intensity *I* and optical field *E* is

$$I = \frac{1}{2} c \varepsilon_0 E^2 \quad (\varepsilon_0 = 8.87 \times 10^{-12}\ \mathrm{F \cdot m^{-1}}) \qquad (4)$$

Then, the general optical field *E* can be obtained

$$E = \sqrt{\frac{2I}{c\varepsilon_0}} = \sqrt{\frac{2 \times 8.85 \times 10^{12}}{3 \times 10^8 \cdot 8.87 \times 10^{-12}}} = 8.16 \times 10^7 V \cdot m^{-1} \qquad (5)$$

In our experiment, the optimum intensity ratio of the two seeding beam was first obtained. If we take the general optical field *E* as the polar optical field approximately, and the NLO molecule of DR-1 has the dipole moment of 8.7D (1 D = 3.334×10-30C·m)[15]. Accordingly, the energy of making NLO molecules orientation by polar optical field can be expressed as

$$\mu E = 8.7 \times 3.334 \times 10^{-30} C \cdot m \bullet 8.16 \times 10^7 V \cdot m^{-1} = 2.36 \times 10^{-21} J \qquad (6)$$

Furthermore, the μE will be kept as constant under different temperature in the all optical poling. Next, the influence of poling temperature on thermodynamic function *U* is considered.

Now, what we do next is to calculate the thermodynamic function *U* of internal energy. Here, we introduced the classical ideal gas model, and the corresponding *U* of ideal gas can be expressed by following partition function [16], which is only related to the thermal motion of molecules.

$$U = NkT^2 \left(\frac{\partial \ln q}{\partial T} \right)_{V,N} = \frac{3}{2} NkT \quad (\mathrm{k} = 1.38 \times 10^{-23}\ \mathrm{J \cdot K^{-1}}) \qquad (7)$$

In fact, the sample is a polymer film, which has significant difference with the ideal gas model. In order to characterize this difference, a "viscosity factor" $\eta = f(N)$ (N is the mole number of the NLO molecule) was first proposed. Thus, the inequation of $\mu E \geq U$ can be expressed as:

$$\mu E \geq \eta \frac{3}{2} kT \qquad (8)$$

From previous analysis, when the poling temperature is at 63℃,a critical point of the energy equilibrium occurs, that means $\mu E = U$, so we can obtain the value of η =0.34 from following equation.

$$\eta \cdot \frac{3}{2} \times 1.38 \times 10^{-23} \times 336.15 = 2.36 \times 10^{-21} \qquad (9)$$

Then, the final condition to realize the all-optical poling for this crosslinked system can be expressed as:

$$\mu E \geq 0.51\,kT \tag{10}$$

3.4 The comparison of decay process of photoinduced SHG

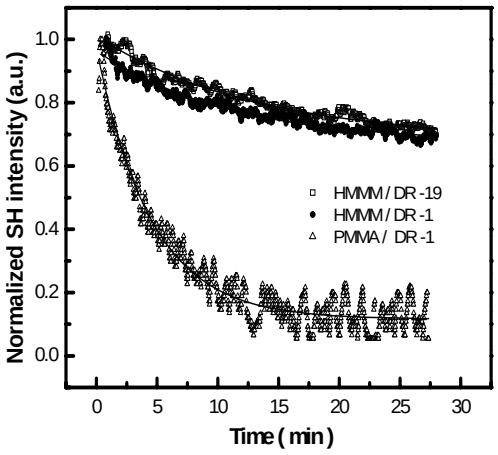

Fig. 5. Decay of normalized photoinduced SHG of HMMM/DR-1, 19 and PMMA/ DR1.

After the photoinduced SHG signal intensity increased to the saturation value, the 2ω beam was blocked and the decay evolution was measured under room temperature. Fig. 5, shows the decay of the normalized SHG induced in PMMA/DR-1 and HMMM/DR-1 and HMMM/DR-19 samples with same thickness of 1μm, it can be found that, after about 27min, 72.3%, 69.1% and 12.3% of the initial value could be maintained in HMMM/DR-19, HMMM/DR-1 and PMMA/DR-1, respectively. This result indicated the temporal stability of HMMM series is much higher than PMMA/DR-1. The reason can be ascribed to the different chemical structure for the two systems, more detailed discussion will be in the next paragraph. For easy to compare, a mono-exponential function (equation 11) was used [17], and the solid lines are the fitting results in Fig. 5.

$$y = A_0 + A\exp\left(-t/\tau_A\right) \tag{11}$$

Table 1. Parameters obtained by fitting the decay curves in Fig. 5 to Eq. (11).*

Sample	A_0 (a.u.)	A (a.u.)	τ_A (min)
DR1-PMMA	0.11578	0.85641	4.50772
HMMM/DR-1	0.67267	0.29203	10.83305
HMMM/DR-19	0.68049	0.33014	13.10693

*The parameters were fitted with Microcal Origin Software.

The fitting parameters are summarized in Table 1. The constant A_0 represents the part of SHG that is due to quasi-permanent net orientation with life-time much larger than τ_A, which is the time constant[15]. It can be seen that both the A_0 and τ_A in HMMM series are larger than in DR1-PMMA. This result could be explained by the cross-linked features in HMMM/DR-19 and HMMM/DR-1, where DR dye was connected covalently with the HMMM matrix, the disorientation of *trans* molecules by thermal diffusion was restricted effectively. However, in PMMA/ DR-1, the chromophore is only simply doped in the polymer matrix and there is no much more limitation in surrounding to restrict its disorientation, so its decay process is much faster. In addition, because of the difference between DR-19 with two hydroxyl groups and DR-1 with one hydroxyl group, HMMM/DR-19 appears a little more stable than HMMM/DR-1 system. From the small differences in A_0 and τ_A between them, we can confirm the standpoint described above.

At last, it should be mentioned that, in organic chromophore incorporated into the PMMA matrices, there appear a substantial influence of the polymer chromophore electrostatic interactions changing charge transfer and contribution of electron-vibration interactions varying the corresponding optical susceptibilities [18]. These factors will be studied fully in our future work.

4. Conclusion

In conclusion, we have investigated the all-optical poling behavior of HMMM/DR-1 and HMMM/DR-19. Optimum poling condition of the two seeding beam intensity ratio, the temperature dependence of all-optical poling process, and the temporal stability of these melamine-based NLO materials were studied in details. It was found the crosslinked HMMM series didn't exhibit the characteristic of thermal-assisted optical poling, and the saturation SHG intensity decreased significantly with the enhanced temperature from 33℃ to 63℃.According to this phenomenon, a relation of the requirement to realize all optical poling was first deduced. Also, a "viscosity factor" η was first proposed, which may be used to characterize the effect on the small molecules from different condensed structure. We hope the simple model will be helpful to understand the mechanism of all-optical poling further.

Acknowledgements

This work was supported by the Open Project (M05003) of Laboratory of Solid State Microstructures, Nanjing University, and National Natural Science Foundation of China (90201016 and 60178030).

References

[1] J. Si, J. Qiu, J. Zhai, Y. Shen, Z. Meng, K. Hirao, J. Appl. Phys. **95**, 3837 (2004).
[2] G. Xu, J. Si, X. Liu, Q. Yang, P. Ye, Z. Li, Y. Shen, Opt. Commun.**153**, 95 (1998).
[3] G. Xu, X. Liu, J. Si, P. Ye, Z. Li, Y. Shen, Appl. Phys.B. **68**, 693 (1999).
[4] J. Si, K. Kitaoka, T. Mitsuyu, P. Ye, K. Hirao, J. Appl. Phys. **85**, 8018 (1999).
[5] R. J. Jeng, G. H. Hsiue, J. I. Chen, S. Marturunkakul, J. Appl. Polym.Sci. **55**, 209 (1995).
[6] G. H. Hsiue, R. H. Lee, R. J. Jeng, Polymer **40**, 6417 (1999).
[7] G. H. Hsiue, W. J. Kuo, C. H. Lin, R. J. Jeng, Macromol. Chem. Phys. **201**, 2336 (2000).
[8] W. J. Kuo, G. H. Hsiue, R. J. Jeng, Macromol. Chem. Phys. **202**, 1782 (2001).
[9] R. C. Wilson, W. F. Pfohl, Vib. Spectrosc. **23**, 13 (2000).
[10] C. Fiorini, F. Charra, J-M. Nunzi, P. Raimond, J. Opt. Soc. Am. B 14, 1984 (1997).
[11] N. Matsuoka, K. Kitaoka, J. Si, K. Fujita, K. Hirao, Opt. Commun. **185**, 467 (2000).
[12] C. Fiorini, J-M. Nunzi, Chem. Phys. Lett. **286**, 415 (1998).
[13] G. Xu, J. Si, X. Liu, Q. Yang, P. Ye, Z. Li, Y. Shen, J. Appl. Phys. **85**, 681 (1999).
[14] X. Liu, G. Xu, J. Si, Q. Yang, P. Ye, Z. Li, Y. Shen, J. Appl. Phys. **88**, 3848 (2000).
[15] H. E. Katz, K. D. Singer, J. E. Sohn, C. W. Dirk, L. A. King, H. M. Gordon, J. Am. Chem. Soc.**109**, 6561 (1987).
[16] X. C. Fu, W. X. Shen, T. Y. Yao, Physical Chemistry, Higher Education Press, Beijing, 1990, (in Chinese).
[17] V. M. Churikov, M. F. Hung, C. C. Hsu, C. W. Shiau, T. Y. Luh, Chem. Phys. Lett. **332**, 19 (2000).
[18] E. Koscien, J. Sanetra, E. Gondek, B. Jarosz, I. V. Kityk, J. Ebothe, A.V. Kityk, Opt. Commun. **242**, 401 (2004).

*Corresponding author: gbm@ustc.edu